ACS Photonics

Letter

pubs.acs.org/journal/apchd5

Amplification of the Evanescent Field of Free Electrons

Jin-Kyu So,*[,†] F. Javier García de Abajo,[†,‡,§] Kevin F. MacDonald,[†] and Nikolay I. Zheludev[†,∥]

[†]Optoelectronics Research Centre & Centre for Photonic Metamaterials, University of Southampton, Southampton SO17 1BJ, U.K.

[‡]ICFO - Institut de Ciencies Fotoniques, Mediterranean Technology Park, Castelldefels, 08860 Barcelona, Spain

[§]ICREA - Institució Catalana de Reserca i Estudis Avançats, Passeig Lluís Campanys 23, 08010 Barcelona, Spain

[∥]The Photonics Institute & Centre for Disruptive Photonic Technologies, Nanyanag Technological University, Singapore 637371, Singapore

Supporting Information

ABSTRACT: Evanescent optical fields existing in close proximity to illuminated objects contain detailed information on length scales smaller than the wavelength. They do not propagate to external observers but can be accessed using negative-index lenses, or coupled to propagating waves via subwavelength apertures, to achieve imaging resolution beyond the diffraction limit. Free electrons moving in vacuum also carry imperceptible localized, visible-frequency evanescent fields, and we demonstrate experimentally here that these fields can be amplified by a plasmonic film as electrons fly over the surface, offering new avenues toward the exploitation of electron evanescent fields for enhanced microscopy and nanoscale light generation. Amplifiers are fabricated at the tips of tapered optical fiber probes decorated with nanogratings to resonantly scatter electron fields to UV/vis light. We record amplification factors up to 3.4 in the ~850 THz (~350 nm) spectral range for medium-energy (40−50 keV) electrons.

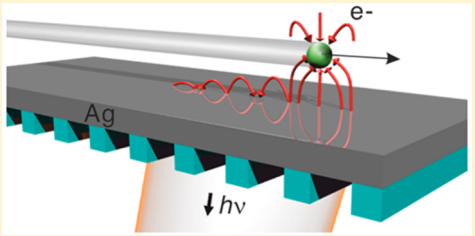

KEYWORDS: *electron beam, plasmonics, evanescent field amplification, Smith−Purcell emission, free-electron light sources*

The amplification of propagating light underpins numerous technologies of fundamental importance to today's society. It is exploited in lasers, which are now deployed ubiquitously in applications ranging from data storage to welding and surgery, as well as in the enormous number of fiber amplifiers that regenerate signals in our global optical telecommunications networks. Exploiting short-range electromagnetic near-fields—nonpropagating evanescent optical waves generated at the boundaries between different media, such as surface plasmon-polariton (SPP) fields occurring at metallic interfaces—is more challenging. They are harnessed in a variety of coupling and sensing devices,[1−4] but the fact that they decay exponentially with distance from a surface makes it difficult to capture the wealth of information that they can carry. Amplifying such fields offers tremendous technological opportunities. Indeed, it is now well established that they can be exploited to enable optical imaging with spatial resolution superior to conventional, diffraction-limited microscopes.[5] Recent years have witnessed demonstrations of evanescent light-field trapping and passive amplification by a thin metal layer (the so-called "poor-man's superlens"),[6,7] as well as active amplification using gain media in much the same way as propagating wave amplification.[8−10]

While it has been known for some time that electron bombardment excites optical frequency SPPs on a metal surface,[11−13] it is less widely appreciated that fast-moving free electrons carry their own evanescent fields, spanning a wide spectral range that extends to high optical frequencies.[14−16] Here we show that these electron evanescent fields can be amplified by a thin metal film in much the same way as evanescent light fields (Figure 1). Amplifiers are fabricated at the tips of tapered optical fiber probes patterned with nanoscale gratings to out-couple the electron fields to UV/vis light propagating in the fiber. We experimentally demonstrate that a nanoscale film of silver can resonantly amplify the optical frequency spectral components of the evanescent field of medium-energy (40−50 keV) electrons by a factor of up to 3.4.

While optical evanescent fields typically require a "slow-wave medium" or dielectric inhomogeneity to be created, the electromagnetic fields associated with the charge of a free electron moving in a straight line are intrinsically evanescent due to their large wave vector;[15] the parallel component $k_{\parallel} = \omega/v$ along the electron velocity vector $\mathbf{v}$ is proportional to the field frequency ω, which should be compared with the wave vector of propagating optical waves ω/c (where c is the speed of light in vacuum), as shown in Figure 2a. This evanescent electron field behaves as an optical evanescent field, with an exponential decay of $\sim\exp(-R\omega/\gamma v)$ in amplitude as a function of distance R from the electron trajectory, where γ is the Lorentz factor $(1 - v^2/c^2)^{-1/2}$. Figure 2b shows the spectral composition of the evanescent field over the visible to near-infrared range at a distance of R = 100 nm from the electron path for a selection of kinetic energies, illustrating the rapid decay of higher frequency components, except for highly relativistic (MeV) energies. It is for this reason that low/

Received: March 18, 2015
Published: August 11, 2015

DOI: 10.1021/acsphotonics.5b00130
ACS Photonics 2015, 2, 1236−1240

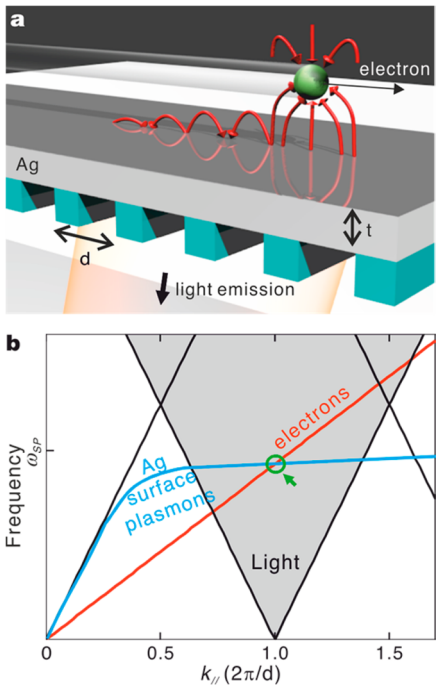

Figure 1. (a) Artistic impression of the electron-evanescent-field plasmonic amplifier. The field associated with passing electrons is amplified by a nanoscale silver layer ($t \sim$ tens of nm) and subsequently coupled to propagating light by the underlying grating. (b) Dispersion relations for surface plasmons on silver (blue) and the evanescent waves of medium-energy free electrons (red). Light lines (black) are shown for the fundamental mode and first diffraction order (shaded) of a grating with period d. Phase velocities are matched at the circled intersection, which is in turn matched to the $k_{\|} = 2\pi/d$ condition for first-order Smith−Purcell light emission in the surface-normal direction via appropriate selection of d.

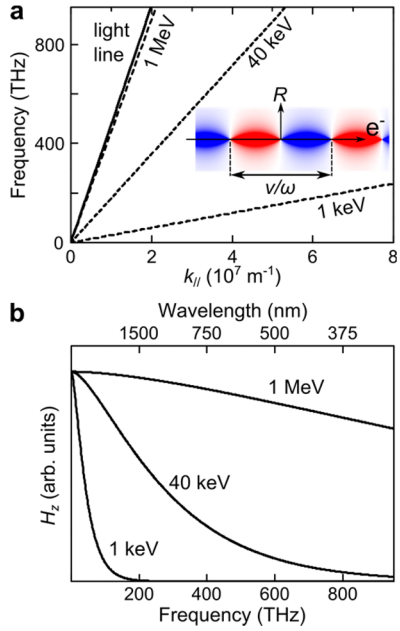

Figure 2. (a) Dispersion relations for light in free space (solid line) and for the evanescent waves of moving free electrons in vacuum at a selection of kinetic energies (dashed, as labeled), $k_{\|}$ being the wave vector component along the electron trajectory. The inset shows an instantaneous map of the radial electric field distribution at fixed frequency ω showing oscillations along the trajectory with spatial wavelength v/ω and evanescent decay as $K_1(\omega R/v\gamma)$ with distance R from the electron trajectory (K_1 being the modified Bessel function of the second kind). (b) Spectral composition of the magnetic evanescent field component along the azimuthal direction relative to the trajectory for an individual electron with a selection of kinetic energy levels (as labeled), evaluated at an impact parameter R = 100 nm.

medium-energy free-electron evanescent fields interact only weakly with nanophotonic systems operating at optical or higher frequencies.

Here, we open up the possibility of directly manipulating the evanescent field of free electrons by demonstrating amplification of this field. By analogy with the poor-man's superlens, wherein the evanescent light-field components emanating from an object are restored by a thin silver layer to image the object with resolution beyond the diffraction limit,[6,7] we employ a silver layer here to amplify the rapidly decaying electron evanescent field.[17−19] In the poor-man's superlens, the optical near-field is amplified across the silver film due to the resonant excitation of surface plasmons on its surfaces at a certain optimum silver thickness. Instead of the optical evanescent field, we consider the field of a free electron moving close to the silver film as the plasmonic excitation source (Figure 1a). Only surface plasmons matching the phase velocity of the moving electron are excited, leading to amplification of the electron evanescent field at the frequency satisfying this condition. This amplified field can be out-coupled to propagating light modes by placing the film either on a "slow-wave medium", in which the speed of light is less than the electron velocity, or near a dielectric inhomogeneity such as a grating. The former gives rise to Cerenkov radiation,[20] whereas the latter produces so-called diffraction or "Smith−Purcell" radiation.[16,21] We adopt the Smith−Purcell configuration, as it is more readily applicable to medium-energy electrons using low-index optical media. By analyzing the electron-induced light emission from a given nanograting with and without an intermediate silver film, we evaluate the magnitude of evanescent field amplification achieved by the film.

Figure 1b illustrates the nature of the coupling from the electron evanescent field to propagating light. Dispersion relations for surface plasmons on a single planar silver/vacuum interface (blue line) and a free-electron evanescent field (red) are shown against the light line and its *umklapp*-images corresponding to a grating period d. The nanograting provides a momentum shift (*umklapp*) in integral multiples of $2\pi/d$, so that some of the electron evanescent waves fall into the diffracted light cone and can thus be out-coupled to propagating light waves. In the absence of the silver film, this simply gives rise to Smith−Purcell radiation at a wavelength $\lambda = (d/n)(\beta^{-1} - \cos\theta)$, where n is the diffraction order, $\beta = v/c$, and θ is the angle between the directions of light emission and electron propagation,[16] a process that is most efficient along the surface-normal direction for low/medium-energy electrons.[22] When the thin silver layer is present, the passing electron excites surface plasmons with the same electron-path-projected phase velocity as the electron, which can in turn be matched with an appropriate choice of grating period to out-couple along the surface-normal direction within the first diffracted light zone at $k_{\|} = 2\pi/d$ (the point indicated with a green circle in Figure 1b). A grating period of 130 nm, which matches the emission of λ = 348 nm light at $\theta = \pm 90°$ for an electron energy of 40 keV, is selected for the present study.

Several practical obstacles must be overcome to enable the experimental observation of light emission amplified in this way

DOI: 10.1021/acsphotonics.5b00130
ACS Photonics 2015, 2, 1236−1240

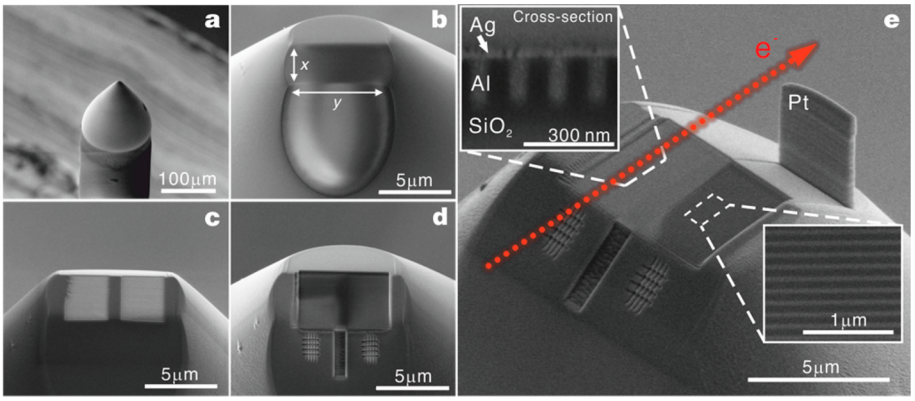

Figure 3. Stages in the fabrication of fiber-probe-mounted electron evanescent field plasmonic amplifiers (scanning electron microscope images): A conically profiled multimode optical fiber tip (a) is truncated to form a device platform (b) into which a matching pair of 130 nm period gratings is etched (c). These are infilled with aluminum and planarized (d) before one of the gratings is coated with a thin silver film deposited at oblique incidence while the second grating is shadowed by a platinum screen (e). Insets show detail of the uncoated silica/aluminum grating (right) and a cross-section of the silver-coated grating (left). The platinum screen is detached before electron-induced light emission experiments are conducted.

by a thin silver film. First, because any electrons impacting the sample will generate a strong cathodoluminescence background signal, one requires either a highly collimated and precisely aligned electron beam to pass uninterrupted over a planar sample or a sample with a microscopic footprint along the electron propagation direction that can approach the waist of a focused electron beam without obstructing its convergent/divergent path. Second, in order to observe the amplifying effect of the silver film, one must detect emitted light from the back side of the grating, the downward direction in Figure 1a, i.e., the opposite of that on which the electron is passing, in contrast to conventional Smith−Purcell configurations. Finally, to unambiguously demonstrate the amplifying effect of the silver film, emission measurements must be obtained for several film thicknesses for any given set of experimental conditions.

We address the first two of these issues by employing conically tapered fiber tips as device platforms that simultaneously serve to present nanograting/silver film devices to the waist of the focused beam of a scanning electron microscope without generating prohibitive levels of cathodoluminescence and as an inherently optimally coupled waveguide to collect light emitted from the back of the grating along the surface-normal direction.[23] The third point above is addressed by manufacturing samples on these probe tips in pairs, with each silver-coated grating lying adjacent to an identical uncoated grating (Figure 3e), such that the two of them can be probed sequentially using the same electron beam parameters. The uncoated gratings thus provide a consistent emission level reference across all samples. The fabrication process for these fiber-probe-mounted amplifier devices is detailed in Figure 3 and the Methods section.

The electron evanescent field "pumping" of fiber-tip-mounted nanograting/amplifier devices was performed in a scanning electron microscope, operating in fixed-spot mode (with a beam waist diameter ∼50 nm and beam current ∼10 nA) at grazing incidence (a notional impact parameter of ∼25 nm) with the grating lines aligned perpendicular to the electron trajectory. Light emitted from the back of the grating in the surface-normal direction is collected by the fiber and delivered to a UV−vis spectrometer equipped with a liquid-nitrogen-cooled CCD array detector. A series of samples, each with the same 130 nm grating period but different silver film thicknesses from 7 to 40 nm, were characterized at electron energies between 40 and 50 keV. Figure 4a shows electron-induced light emission spectra (cathodoluminescence background subtracted[23]) for nanogratings with and without an intermediate 15 nm silver layer at a selection of electron energies. The amplifying effect of the silver film can clearly be observed in the variation with electron energy of differences between coated and uncoated grating spectra. Due to the phase-velocity matching condition between surface plasmons and free electrons, there exists an optimum electron energy for evanescent field enhancement, found to be 42 keV in the

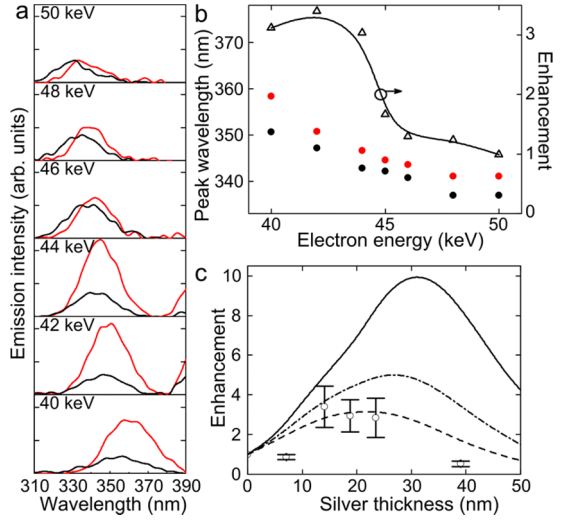

Figure 4. (a) Electron-induced light emission spectra from 130 nm period gratings with (red) and without (black) a 15 nm silver film at electron energies between 40 and 50 keV (as labeled, all on identical vertical scales). (b) Peak emission wavelength (red and black dots for gratings with and without the silver amplifier layer, respectively) and emission intensity enhancement delivered by the silver film (open triangles) as functions of electron energy. (c) Emission intensity enhancement (open circles) as a function of silver film thickness at the experimental optimum electron energy of 42 keV against curves derived from a particle-in-cell numerical simulation of the amplifier-grating system at the corresponding numerical optimum of 46 keV (see Supporting Information), wherein the silver permittivity is described by a Drude model assuming collision frequencies $\gamma_c = 8.35 \times 10^{13}$ Hz (solid line), $2\gamma_c$ (dash-dot), and $3\gamma_c$ (dashed).

DOI: 10.1021/acsphotonics.5b00130
ACS Photonics 2015, 2, 1236−1240

present case, for which an emission intensity enhancement of a factor of 3.4 is obtained. This enhancement factor (Figure 4b) decreases at higher electron energies, falling to 1 (i.e., no enhancement) at ∼50 keV. It is also expected to decrease at lower electron energies, but this trend was not observable against the rapidly increasing background of cathodoluminescence emission from silica at longer wavelengths.

The experimental data show a clear blue shift in the peak emission wavelength with increasing electron energy for both coated and uncoated gratings (peak position being plotted as a function of electron energy in Figure 4b). In the Smith−Purcell effect the surface-normal emission wavelength is inversely proportional to electron velocity (i.e., to the phase velocity of the electron evanescent field). The fact that there is a concomitant shift in the emission peak wavelengths for the silver-coated gratings indicates that the amplified emission shares the same origin. Alternative emission mechanisms, such as electron impact on the sample, show no such spectral dependence on electron energy. The offset between spectra for coated and uncoated nanogratings at a given electron energy—the former being consistently red-shifted with respect to the latter—is attributed to the nature of the coupling between electron evanescent fields and nanogratings via surface plasmons on the silver film (see further discussion in the Supporting Information).

The observed light emission intensity enhancement also exhibits a dependence on the silver film thickness, as shown in Figure 4c. The measured enhancement factor at a peak wavelength of ∼350 nm for 42 keV electrons reaches a maximum at a thickness of 15 nm, decreasing for thicker films due to losses in the silver. The quality of the silver film is also important. The experimental data are plotted alongside a family of curves derived from a model in which silver is described by Drude permittivities with three different values of the inelastic attenuation rate ($\gamma_c = 8.35 \times 10^{13}$ Hz [ref 24], $2\gamma_c$, and $3\gamma_c$) in order to mimic the increase in optical losses with decreasing film quality.[25,26] The maximum achievable enhancement and corresponding optimum film thickness both decrease with increasing losses (i.e., enhancement factors greater than the experimentally observed value of 3.4 may be obtained through optimization of the silver film deposition process).

In summary, we present an experimental demonstration of the fact that the evanescent optical field of free electrons traveling in vacuum can be amplified via a thin plasmonic metal film akin to the so-called poor-man's superlens for optical evanescent fields. This is enabled by the resonant excitation of traveling surface plasmons on the metal film through proximity interaction with moving electrons. Our findings consolidate the picture of a moving electron as a broadband evanescent electromagnetic wave source, paving the way for the many disruptive concepts proposed for optical near-field manipulation in nanophotonics to be applied to free-electron interactions. This scenario thereby offers novel approaches to areas as varied as the realization of electron-beam-based tunable light sources;[27−29] laser-driven and plasmon-assisted particle accelerators;[30−32] charged particle beam diagnostics (e.g., highly accurate yet minimally invasive sensing of beam position, geometry, and temporal profile, as required for the tuning of high-energy accelerators[33,34]); electron energy loss and gain spectroscopies (EELS/EEGS);[35,36] near-field manipulation of the free-electron wave function along its direction of motion;[37] and a new form of microscopy whereby samples are imaged through the protective shielding of the amplifying metal film. The interaction mechanism can be engaged across a broad spectral range, subject to the appropriate engineering of nanostructures, while the fiber-based probe configuration can serve as a versatile platform for the interrogation of proximity interactions between free electrons and a wide variety of nanophotonic structures. The concepts put forward in this work can be readily extended to other evanescent field amplifying structures, such as planar dielectric waveguides and optical micro/nanoresonators.

METHODS

Fabrication of Fiber-Probe-Mounted Electron Evanescent Field Plasmonic Amplifier Samples. One end of a multimode optical fiber (Thorlabs SFS50/125Y) is conically profiled using a laser fiber processor (OpTek). This is coated with a 40 nm thick chromium film by electron beam evaporation to prevent charging during the process of truncation by focused ion beam (FIB) milling (FEI Helios NanoLab 600 DualBeam) to form an exposed silica platform perpendicular to the fiber axis that has a uniform length x (parallel to the intended electron beam path, on the order of 5 μm) across its full width y (see Figure 3b). The fiber is then coated again with a 40 nm thick chromium film, and gratings with a period of 130 nm along x are milled by FIB into the platform to a depth on the order of 300 nm. A thick aluminum film is deposited by electron beam evaporation to fill in the newly formed lines of the grating, and the fiber tip is then planarized by FIB to expose a matched pair of silica/aluminum gratings (with a typical remaining depth of ∼150 nm). In order to enable selective deposition of silver over one of these two gratings, a platinum screen is raised in front of the other by electron-beam-induced deposition to act as a shadow mask during the oblique incidence deposition of silver by evaporation (to obtain continuous silver films, a 1 nm germanium wetting layer was deposited first[38]). Finally, the screen is mechanically detached using a piezoelectrically controlled micromanipulator tip.

ASSOCIATED CONTENT

Supporting Information

The Supporting Information is available free of charge on the ACS Publications website at DOI: 10.1021/acsphotonics.5b00130.

Further information on 2D numerical modeling of the electron evanescent field amplifier (PDF)

Following a period of embargo, the data from this paper can be obtained from the University of Southampton ePrints research repository, DOI: 10.5258/SOTON/380394.

AUTHOR INFORMATION

Corresponding Author

*E-mail: js1m10@orc.soton.ac.uk.

Notes

The authors declare no competing financial interest.

ACKNOWLEDGMENTS

This work was supported by the Engineering and Physical Sciences Research Council, UK [Project EP/G060363/1] (all authors), The Royal Society, and the Singapore Ministry of Education [grant MOE2011-T3-1-005] (N.I.Z.). The authors would like to thank Giorgio Adamo and Jun-Yu Ou for

DOI: 10.1021/acsphotonics.5b00130
ACS Photonics 2015, 2, 1236−1240

constructive discussions respectively on EIRE spectroscopy and FIB processing.

REFERENCES

(1) Ozbay, E. Plasmonics: Merging Photonics and Electronics at Nanoscale Dimensions. *Science* **2006**, *311*, 189−193.
(2) Gramotnev, D. K.; Bozhevolnyi, S. I. Plasmonics Beyond the Diffraction Limit. *Nat. Photonics* **2010**, *4*, 83−91.
(3) Homola, J.; Yee, S. S.; Gauglitz, G. Surface Plasmon Resonance Sensors: Review. *Sens. Actuators, B* **1999**, *54*, 3−15.
(4) Nie, S.; Emory, S. R. Probing Single Molecules and Single Nanoparticles by Surface-Enhanced Raman Scattering. *Science* **1997**, *275*, 1102−1106.
(5) Betzig, E.; Trautman, J.; Harris, T.; Weiner, J.; Kostelak, R. Breaking the Diffraction Barrier: Optical Microscopy on a Nanometric Scale. *Science* **1991**, *251*, 1468−1470.
(6) Pendry, J. B. Negative Refraction Makes a Perfect Lens. *Phys. Rev. Lett.* **2000**, *85*, 3966−3969.
(7) Fang, N.; Lee, H.; Sun, C.; Zhang, X. Sub-Diffraction-Limited Optical Imaging with a Silver Superlens. *Science* **2005**, *308*, 534−537.
(8) Bergman, D. J.; Stockman, M. I. Surface Plasmon Amplification by Stimulated Emission of Radiation: Quantum Generation of Coherent Surface Plasmons in Nanosystems. *Phys. Rev. Lett.* **2003**, *90*, 027402.
(9) Oulton, R. F.; Sorger, V. J.; Zentgraf, T.; Ma, R.-M.; Gladden, C.; Dai, L.; Bartal, G.; Zhang, X. Plasmon Lasers at Deep Subwavelength Scale. *Nature* **2009**, *461*, 629−632.
(10) Zheludev, N. I.; Prosvirnin, S.; Papasimakis, N.; Fedotov, V. Lasing Spaser. *Nat. Photonics* **2008**, *2*, 351−354.
(11) Ritchie, R. H. Plasma Losses by Fast Electrons in Thin Films. *Phys. Rev.* **1957**, *106*, 874−881.
(12) Bashevoy, M.; Jonsson, F.; Krasavin, A.; Zheludev, N.; Chen, Y.; Stockman, M. Generation of Traveling Surface Plasmon Waves by Free-Electron Impact. *Nano Lett.* **2006**, *6*, 1113−1115.
(13) Van Wijngaarden, J.; Verhagen, E.; Polman, A.; Ross, C.; Lezec, H.; Atwater, H. Direct Imaging of Propagation and Damping of near-Resonance Surface Plasmon Polaritons Using Cathodoluminescence Spectroscopy. *Appl. Phys. Lett.* **2006**, *88*, 221111−221111−3.
(14) Di Francia, G. T. On the Theory of Some Čerenkovian Effects. *Nuovo Cimento* **1960**, *16*, 61−77.
(15) García de Abajo, F. J. Optical Excitations in Electron Microscopy. *Rev. Mod. Phys.* **2010**, *82*, 209−275.
(16) Smith, S. J.; Purcell, E. M. Visible Light from Localized Surface Charges Moving across a Grating. *Phys. Rev.* **1953**, *92*, 1069−1069.
(17) Chuang, S.; Kong, J. Enhancement of Smith−Purcell Radiation from a Grating with Surface-Plasmon Excitation. *J. Opt. Soc. Am. A* **1984**, *1*, 672−676.
(18) So, J.-K.; Ou, J.-Y.; Adamo, G.; MacDonald, K. F.; García de Abajo, F. J.; Zheludev, N. I. Amplification of the Evanescent Field of Free Electrons. *Conference on Lasers and Electro-Optics 2012* **2012**, QTh3F.1.
(19) Ping, Z.; Ya-Xin, Z.; Jun, Z.; Wei-Hao, L.; Ren-Bin, Z.; Sheng-Gang, L. Enhancement of Smith−Purcell Radiation with Surface-Plasmon Excitation. *Chin. Phys. B* **2012**, *21*, 104102.
(20) Jelley, J. V. *Cerenkov Radiation and Its Applications*; Pergamon Press: London, 1958.
(21) Muto, T.; Araki, S.; Hamatsu, R.; Hayano, H.; Hirose, T.; Karataev, P.; Naumenko, G.; Potylitsyn, A.; Urakawa, J. Observation of Incoherent Diffraction Radiation from a Single-Edge Target in the Visible-Light Region. *Phys. Rev. Lett.* **2003**, *90*, 104801.
(22) Trotz, S. R.; Brownell, J.; Walsh, J. E.; Doucas, G. Optimization of Smith-Purcell Radiation at Very High Energies. *Phys. Rev. E: Stat. Phys., Plasmas, Fluids, Relat. Interdiscip. Top.* **2000**, *61*, 7057.
(23) So, J. K.; MacDonald, K. F.; Zheludev, N. I. Fiber Optic Probe of Free Electron Evanescent Fields in the Optical Frequency Range. *Appl. Phys. Lett.* **2014**, *104*, 201101.
(24) Sweatlock, L. A.; Maier, S. A.; Atwater, H. A.; Penninkhof, J. J.; Polman, A. Highly Confined Electromagnetic Fields in Arrays of Strongly Coupled Ag Nanoparticles. *Phys. Rev. B: Condens. Matter Mater. Phys.* **2005**, *71*, 235408.
(25) Kuttge, M.; Vesseur, E.; Verhoeven, J.; Lezec, H.; Atwater, H.; Polman, A. Loss Mechanisms of Surface Plasmon Polaritons on Gold Probed by Cathodoluminescence Imaging Spectroscopy. *Appl. Phys. Lett.* **2008**, *93*, 113110.
(26) Chen, K.-P.; Drachev, V. P.; Borneman, J. D.; Kildishev, A. V.; Shalaev, V. M. Drude Relaxation Rate in Grained Gold Nanoantennas. *Nano Lett.* **2010**, *10*, 916−922.
(27) Urata, J.; Goldstein, M.; Kimmitt, M.; Naumov, A.; Platt, C.; Walsh, J. Superradiant Smith-Purcell Emission. *Phys. Rev. Lett.* **1998**, *80*, 516.
(28) Jin, Z.; Chen, Z.; Zhuo, H.; Kon, A.; Nakatsutsumi, M.; Wang, H.; Zhang, B.; Gu, Y.; Wu, Y.; Zhu, B. Tunable Radiation Source by Coupling Laser-Plasma-Generated Electrons to a Periodic Structure. *Phys. Rev. Lett.* **2011**, *107*, 265003.
(29) Cook, A.; Tikhoplav, R.; Tochitsky, S. Y.; Travish, G.; Williams, O.; Rosenzweig, J. Observation of Narrow-Band Terahertz Coherent Cherenkov Radiation from a Cylindrical Dielectric-Lined Waveguide. *Phys. Rev. Lett.* **2009**, *103*, 095003.
(30) Breuer, J.; Hommelhoff, P. Laser-Based Acceleration of Nonrelativistic Electrons at a Dielectric Structure. *Phys. Rev. Lett.* **2013**, *111*, 134803.
(31) Peralta, E.; Soong, K.; England, R.; Colby, E.; Wu, Z.; Montazeri, B.; McGuinness, C.; McNeur, J.; Leedle, K.; Walz, D. Demonstration of Electron Acceleration in a Laser-Driven Dielectric Microstructure. *Nature* **2013**, *503*, 91−94.
(32) Saito, N.; Ogata, A. Plasmon Linac: A Laser Wake-Field Accelerator Based on a Solid-State Plasma. *Phys. Plasmas* **2003**, *10*, 3358−3362.
(33) Inoue, Y.; Hayano, H.; Honda, Y.; Takatomi, T.; Tauchi, T.; Urakawa, J.; Komamiya, S.; Nakamura, T.; Sanuki, T.; Kim, E.-S. Development of a High-Resolution Cavity-Beam Position Monitor. *Phys. Rev. Spec. Top.–Accel. Beams* **2008**, *11*, 062801.
(34) Soong, K.; Peralta, E. A.; Joel England, R.; Wu, Z.; Colby, E. R.; Makasyuk, I.; MacArthur, J. P.; Ceballos, A.; Byer, R. L. Electron Beam Position Monitor for a Dielectric Microaccelerator. *Opt. Lett.* **2014**, *39*, 4747−4750.
(35) García de Abajo, F. J.; Kociak, M. Electron Energy-Gain Spectroscopy. *New J. Phys.* **2008**, *10*, 073035.
(36) Asenjo-Garcia, A.; García de Abajo, F. J. Plasmon Electron Energy-Gain Spectroscopy. *New J. Phys.* **2013**, *15*, 103021.
(37) Feist, A.; Echternkamp, K. E.; Schauss, J.; Yalunin, S. V.; Schäfer, S.; Ropers, C. Quantum Coherent Optical Phase Modulation in an Ultrafast Transmission Electron Microscope. *Nature* **2015**, *521*, 200−203.
(38) Chen, W.; Thoreson, M. D.; Ishii, S.; Kildishev, A. V.; Shalaev, V. M. Ultra-Thin Ultra-Smooth and Low-Loss Silver Films on a Germanium Wetting Layer. *Opt. Express* **2010**, *18*, 5124−5134.

DOI: 10.1021/acsphotonics.5b00130
ACS Photonics 2015, 2, 1236−1240